Biconvex Optimization for Time-Domain Channel Estimation under Dual-Wideband Fading Conditions

Evangelos Vlachos[1] and George C. Alexandropoulos[2]
[1]Industrial Systems Institute, ATHENA Research Center, Patras, Greece; evlachos@athenarc.gr
[2]Dept. of Informatics and Telecommunications, National Technical University of Athens, Greece; alexandg@di.uoa.gr

***Abstract*—Single-carrier (SC) waveforms offer significant advantages in high-frequency communications due to their lower peak-to-average power ratios, mitigating channel and system impairments. While extensive research has addressed dual-wideband fading challenges for OFDM systems in mmWave/THz, the investigation of these effects in SC MIMO transmissions remains limited. This paper focuses on the time-domain estimation of MIMO channel matrices for point-to-point systems under dual-wideband fading, encompassing both beam squint and inter-symbol interference (ISI). We propose a unified framework that accounts for beam squint at both the transmitter and receiver, as well as ISI caused by propagation delays, addressing limitations prevalent in single-antenna studies. A novel mixed-integer biconvex model provides a flexible channel estimation framework. It handles diverse delay patterns using a binary vector and decomposes the channel into path-specific matrices for smart environment integration, such as sensing and reflecting surfaces. This semi-parametric approach, estimating delays and separating path gains/angles, offers advantages over conventional methods and enables advanced optimization.**

***Index Terms*—MIMO channel estimation, dual-wideband, beam-squint, intersymbol interference, single-carrier, mmWave**

I. Introduction

The predominant literature for channel estimation in high-frequency communications, i.e., millimeter wave (mmWave) and terahertz (THz), with a specific focus on the beam-squint effect revolves around schemes relying on Orthogonal Frequency Division Multiplexing (OFDM). In [1], the authors presented a parametric channel estimator where the delay and angles were derived for all the subcarriers. While this approach simplifies the estimation problem, careful selection of parameters is crucial to avoid ill-conditioning and potential divergence from the solution. In [2], the dual-wideband effect was addressed for mmWave multiple-input multiple-output (MIMO) OFDM for parametric channel estimation. To avoid unstable initialization, the approach relied on tensor-based modeling and problem decomposition. A scenario with single-antenna multiple users was addressed in [3], where the channel parameters were obtained via the maximum a posteriori criterion. An adaptive deep learning approach for THz XL MIMO channel estimation was proposed in [4]. To mitigate wideband effects, the authors suggest extending their technique by employing parallel streams for each subcarrier, leveraging the learned codebooks. However, given that mmWave/THz systems will have large bandwidths, and thus, many subcarriers, this approach could lead to very high computational complexity.

Single-carrier (SC) waveforms are known for having lower peak-to-‘ ratios compared to OFDM which makes them robust to channel-induced and system impairments. Especially for high-frequency communications, due to the low output power and the non-linearity effect induced by the available power amplifiers (PAs), it is preferable to use SC transmissions rather than OFDM [5], [6], [7], [8], [9], [10]. In [5], hybrid precoding for the wideband millimiter wave communications is considered, proposing a SC-based sparse optimization technique. The authors in [6] claim that SC modulation with time-domain equalization, which exhibits the smallest loss concerning the non-linear distortions due to the PAs. In [9], an SC sparsity-based algorithm was proposed for indoor THz channel estimation, which incorporated high molecular absorption, but did not consider MIMO systems neither the spatial wideband effect. Moreover, IEEE 802.15.3d standard for the sub-THz 6G communications, supports SC mode for high data rate applications [11].

A. Motivation and Contributions

Although the problem of dual-wideband fading (i.e., intersymbol interference and beam squint) for channel estimation have been extensively studied for OFDM systems in mmWave/THz communications, the investigation of the former on single-carrier MIMO transmissions has been significantly limited [8]. In this paper, we focus on the general estimation problem of MIMO channel matrices for point-to-point systems in the time-domain subject to dual-wideband fading conditions. A unified framework is proposed accounting for beam-squint effects at both the transmitter (TX) and receiver (RX), as well as inter-symbol interference caused by propagation path delays—limitations often overlooked in single-antenna user studies. A novel mixed-integer biconvex model introduces a versatile channel estimation framework. It effectively manages diverse delay patterns through binary vector representation and decomposes the channel into path-specific matrices, facilitating seamless integration with smart environments, including sensing and reflecting surfaces. This semi-parametric approach explicitly estimates delays while isolating path gains and angles, providing significant advantages over traditional methods and enabling the use of sophisticated optimization techniques.

II. System and Channel Models

We consider a point-to-point THz MIMO communication system comprising an N-antenna base station (BS) and an M-antenna user equipment (UE). The antenna elements at both nodes are structured in ULAs and, for their data communication, SC transmissions are adopted over a designated carrier frequency f_c resulting in wavelength $\lambda_c = c/f_c$ with c the speed of light, a bandwidth W, and a corresponding sampling period $T_s = 1/(2W)$.

A. Wideband Channel Time-Domain Model

While the prevalent trend in mmWave/THz channel modeling literature typically involves Line-of-Sight (LoS)-dominant scenarios [12], it is essential to recognize that multipath wideband channels may emerge in various scenarios [13], especially within smart wireless environments featured by reconfigurable metasurfaces [14].

To model multipath $M \times N$ MIMO wireless channels, we adopt the Saleh-Valenzuela channel model that is based on the time-cluster spatial-lobe approach [15]. To this end, the t-th time instance *effective* channel – which includes the propagation and the TX-RX filters – between each n-th transmit and each m-th receive antennas, with $t = 1, 2, \ldots, T$, $n = 1, 2, \ldots, N$ and $m = 1, 2, \ldots, M$, is given by the discrete time baseband model [16]:

$$h_{m,n}(t) = \sqrt{g} \sum_{\ell=1}^{L_p} \tilde{a}_\ell e^{-j2\pi d_{m,n,\ell}/\lambda_c} \delta(t - \tilde{\tau}_{m,n,\ell}), \quad (1)$$

where $\sqrt{g}$ is the product of the transmit and receive antenna field radiation patterns in the LoS direction, L_p is the number of resolvable propagation paths due to multipath propagation; $\tilde{\tau}_{m,n,\ell} \triangleq \frac{\tilde{d}_{m,n,\ell}}{c}$ is the total propagation time delay of the ℓ-th channel path ($\ell = 1, \ldots, L_p$) between the m-th receiving and n-th transmitting antennas; $\tilde{d}_{m,n,\ell}$ is the distance between these antennas for the ℓ-th propagation path, and $\tilde{\alpha}_\ell$ is the instantaneous channel gain for the ℓ-th path.

In the context of far-field communications, where the antenna array sizes are significantly smaller than the distances between them, the total separation between the n-th transmit antenna and the m-th receive antenna can be effectively approximated. This approximation involves summing the distance from the first transmit antenna to the first receive antenna, denoted as $d_{\text{TX-RX}}$, and the additional distance attributed to the signal's travel on the aperture, denoted as $d_{m,n,\ell}$. Specifically, this approximation is expressed as follows:

$$\tilde{d}_{m,n,\ell} = d_{\text{TX-RX}} + d_{m,n,\ell}, \quad (2)$$

and consequently the propagation time delay is expressed as:

$$\tilde{\tau}_{\text{TOTAL}} = \tau_{\text{TX-RX}} + \tau_{m,n,l}. \quad (3)$$

The travel distance on the uniform linear array (ULA) aperture is defined as:

$$d_{m,n,\ell} \triangleq (m-1)\Delta_c \cos\vartheta_{\text{TX},\ell} - (n-1)\Delta_c \cos\vartheta_{\text{RX},\ell} \quad (4)$$

with $\Delta_c = \frac{\lambda_c}{2} = \frac{c}{2f_c}$ denoting the antenna separation and $\vartheta_{\text{TX},\ell}, \vartheta_{\text{RX},\ell} \in [-\pi/2, \pi/2]$ are the physical azimuth angles of arrival and departure, respectively, for a ULA. Putting all above together, the MIMO channel representation in (1) becomes:

$$h_{m,n}(t) = \sum_{\ell=1}^{L_p} a_\ell \underbrace{e^{-j2\pi(m-1)\theta_{\text{RX},\ell}} e^{j2\pi(n-1)\theta_{\text{TX},\ell}}}_{\triangleq c_{m,n,\ell}} \delta(t - \tilde{\tau}_{m,n,\ell}) \quad (5)$$

with $\alpha_\ell \triangleq \sqrt{g}\tilde{\alpha}_\ell e^{-j2\pi d_{\text{TX-RX}}/\lambda_c}$, $\theta_{\text{RX},\ell} \triangleq \Delta_c \cos(\vartheta_{\text{RX},\ell})$ is the normalized angle-of-arrival (AoA) and $\theta_{\text{TX},\ell} \triangleq \Delta_c \cos(\vartheta_{\text{TX},\ell})$ is the normalized angle-of-departure (AoD).

In lower frequency ranges, in contrast to mmWave and THz, and in non-extreme MIMO systems, the carrier frequency f_c does not become significantly small and the antenna index m does not reach excessively large values, thus, the delay $\tau_{m,n,\ell}$ becomes negligible. However, for MIMO systems, $\tau_{m,n,\ell}$ shifts the sampling of the transmitted signal, creating the beam-squint effect, where different RX antennas may sample different transmitted symbols. This sampling shift depends on the propagation distance $d_{m,n,\ell}$, between the n-th TX and m-th RX antenna elements, along the ℓ-th path.

Note that $\tau_{m,n,\ell} \in \mathbb{R}$ describes the combined beam-squint effect at the TX and RX. More specifically, this delay is given by the expression:

$$\tau_{m,n,\ell} = \left((m-1)\frac{1}{2f_c}\cos\vartheta_{\text{RX},\ell} - (n-1)\frac{1}{2f_c}\cos\vartheta_{\text{TX},\ell} \right). \quad (6)$$

Since, the AoA and AoD of each ℓ-th propagation path are bounded within $[-\pi/2, \pi/2]$, thus, $\cos\vartheta_{\text{RX},\ell}, \cos\vartheta_{\text{TX},\ell} \in [0, 1]$, the aperture delay time can be upper bounded as follows:

$$\tau_{m,n,\ell} \leq \frac{m-1}{2f_c} + \frac{n-1}{2f_c} \leq \frac{M+N-2}{2f_c}. \quad (7)$$

To avoid beam-squint, the sampling period needs to be chosen to upper bound the propagation delay time, i.e., $\tau_{m,n,\ell} < T_s$. This setting also sets an upper bound for the number of antenna elements that will not be affected from the spatial wideband effect, i.e., it must hold that $\tau_{m,n,\ell} < T_s \Rightarrow \frac{M+N-2}{2f_c} < T_s \Rightarrow M + N < \lceil 2f_c T_s + 2 \rceil$. For instance, with a 150 GHz carrier frequency and 10 GHz bandwidth, implying a $T_s = 5 \times 10^{-11}$ sec (50 psec) sampling period, limiting the combined number of TX and RX antenna elements to $M + N = 16$ will mitigate the beam-squint effect. Inevitable, the use of larger antenna arrays introduces the beam-squint effect, posing a considerable challenge in the design of wideband systems.

III. Proposed Channel Estimation

A. Received Signal Model for Dual-Wideband Fading

The considered point-to-point MIMO communication takes place on a frame-by-frame basis, where the wireless channel remains constant during each frame but may change independently from one frame to another. Every frame consists of T time slots, with $t = 1, 2, \ldots, T$, dedicated for channel estimation, whereas the rest of the frame is used for data

communication. When the TX sends the symbol $q_n(t) \in \mathbb{C}$ from n-th antenna, the noiseless reception at the m-th RX antenna can be expressed as follows [16]:

$$\hat{y}_{m,n}(t) = \sum_{\ell=1}^{L_p} \alpha_\ell c_{m,n,\ell} q_n(t - \tau_{m,n,\ell}), \tag{8}$$

where to ensure causality, it is considered that $t > \tau_{m,n,\ell}$,

Note that, the involved time-varying signals are discrete, thus, the time instance t is an integer, denoting the factor that multiplies the sampling period T_s, i.e., $T_s, 2 \cdot T_s \ldots, T \cdot T_s$. Similarly, the delay $\tau_{m,n,\ell} \in \mathbb{I}$ is an integer factor that multiplies the sampling period, shifting the sampling instance, where $\mathbb{I}$ denotes the set of integers. For notational simplicity, T_s is implicitly assumed in our formulations.

B. Problem Formulation

The introduced time delays pose a significant challenge for estimating the channel impulse response, as it's particularly difficult to accurately determine the propagation delays for every transmit-receive antenna pair. Our proposed formulation effectively transforms the problem into a sparse estimation task by expressing each time-shifted training symbol as an inner product of a fixed vector and a binary vector.

Proposition 1. *Considering that time instance t and the delay $\tau_{m,n,\ell}$ are integers, then each shifted training symbol can be equivalently expressed as:*

$$q_n(t - \tau_{m,n,\ell}) \triangleq \mathbf{q}_n^T(t)\mathbf{e}_{\tau_{m,n,\ell}}, \tag{9}$$

where $\mathbf{e}_{m,n,\ell} \in \{0,1\}^{K\times 1}$ is a $K \times 1$ binary vector with zeros everywhere except the $\tau_{m,n,\ell}$-th position, i.e., $\|\mathbf{e}_{m,n,\ell}\|_0 = 1$; $K \triangleq max(\tau_{m,n,\ell})$, and

$$\mathbf{q}_n(t) \triangleq [q_n(t-K+1), \ldots, q_n(t)]^{\mathrm{T}} \in \mathbb{C}^{K\times 1}. \tag{10}$$

Based on the Proposition 1, the signal $\hat{y}_{m,n}(t)$ in (8) can be rewritten as follows:

$$\hat{y}_{m,n}(t) = \sum_{\ell=1}^{L_p} \alpha_\ell c_{m,n,\ell} q_n(t - \tau_{m,n,\ell}) \tag{11}$$

$$= \sum_{\ell=1}^{L_p} \alpha_\ell c_{m,n,\ell} \mathbf{q}_n^{\mathrm{T}}(t)\mathbf{e}_{m,n,\ell}. \tag{12}$$

While the symbol vector $\mathbf{q}_n(t) \in \mathbb{C}^{K\times 1}$ is known at the RX, the binary vector $\mathbf{e}_{m,n,\ell}$ has to be recovered for all TX and RX antenna elements (recall that $n = 1, 2, \ldots, N$ and $m = 1, 2, \ldots, M$) as well as for all channel propagation paths $\ell = 1, 2, \ldots, L_p$. Equivalently, using vector form expressions to replace the summation, we get:

$$\hat{y}_{m,n}(t) = \mathbf{k}_{m,n}^{\mathrm{T}} \mathbf{Q}_n(t)\mathbf{e}_{m,n}, \tag{13}$$

where we have used the definitions $\mathbf{Q}_n(t) \triangleq (\mathbf{I}_{L_p} \otimes \mathbf{q}_n^{\mathrm{T}}(t)) \in \mathbb{C}^{L_p \times L_p K}$ and

$$\mathbf{e}_{m,n} \triangleq [\mathbf{e}_{m,n,1}^{\mathrm{T}}, \ldots, \mathbf{e}_{m,n,L_p}^{\mathrm{T}}]^{\mathrm{T}} \in \{0,1\}^{L_p K\times 1}. \tag{14}$$

Note that, the channel vector $\mathbf{k}_{m,n} \in \mathbb{C}^{L_p\times 1}$ includes the vectorized values of the channel gains for all L_p paths, which is defined as:

$$\mathbf{k}_{m,n} \triangleq [\alpha_1 c_{m,n,1}, \ldots, \alpha_L c_{m,n,L_p}]^{\mathrm{T}} \in \mathbb{C}^{L_p\times 1}.$$

The noiseless received signal for all TX antennas is given by the superposition $\hat{y}_m(t) = \sum_{n=1}^{N} \hat{y}_{m,n}(t)$. Using (13), this baseband signal can be re-expressed as follows:

$$\hat{y}_m(t) = \sum_{n=1}^{N} \mathbf{k}_{m,n}^{\mathrm{T}} \mathbf{Q}_n(t)\mathbf{e}_{m,n} = \mathbf{k}_m^{\mathrm{T}} \bar{\mathbf{Q}}(t)\mathbf{e}_m, \tag{15}$$

where, for the vectorized expression, we have defined the following quantities:

$$\bar{\mathbf{Q}}(t) \triangleq \mathrm{blkdiag}(\mathbf{Q}_1(t), \ldots, \mathbf{Q}_N(t)) \in \mathbb{C}^{L_p N\times L_p NK}, \tag{16}$$

$$\mathbf{e}_m \triangleq [\mathbf{e}_{m,n}^{\mathrm{T}}, \ldots, \mathbf{e}_{m,N}^{\mathrm{T}}]^{\mathrm{T}} \in \{0,1\}^{L_p KN\times 1}, \tag{17}$$

$$\mathbf{k}_m \triangleq [\mathbf{k}_{m,1}^{\mathrm{T}}, \ldots, \mathbf{k}_{m,N}^{\mathrm{T}}]^{\mathrm{T}} \in \mathbb{C}^{NL_p\times 1}. \tag{18}$$

Next, for each training instance $t = 1, \ldots, T$, we construct the receiving vector $\mathbf{y}(t) \in \mathbb{C}^{M\times 1}$ with the received training symbols from all the M RX antennas, as follows:

$$\mathbf{y}(t) = \mathbf{K}(\mathbf{I}_M \otimes \bar{\mathbf{Q}}(t))\mathbf{e} + \mathbf{n}(t), \tag{19}$$

with

$$\mathbf{K} \triangleq \mathrm{blkdiag}(\mathbf{k}_1^{\mathrm{T}}, \ldots, \mathbf{k}_M^{\mathrm{T}}) \in \mathbb{C}^{M\times MNL_p}, \tag{20}$$

$$\mathbf{e} \triangleq [\mathbf{e}_1^{\mathrm{T}}, \ldots, \mathbf{e}_M^{\mathrm{T}}]^{\mathrm{T}} \in \{0,1\}^{MNLK\times 1}, \tag{21}$$

$\mathbf{I}_M \otimes \bar{\mathbf{Q}}(t)$ is an $MNL_p \times MNLK$ matrix, and $\mathbf{n}(t) \sim \mathcal{N}(\mathbf{0}_M, \sigma^2\mathbf{I}_M)$.

Gathering T training instances, the input/output relationship for the considered $M \times N$ MIMO system over an L_p-tap multipath and wideband channel subject to the combined effects of maximum delay K can be expressed as:

$$\mathbf{Y} = \mathbf{K}\mathbf{\Phi}\mathbf{E} + \mathbf{N}, \tag{22}$$

where $\mathbf{Y} \in \mathbb{C}^{M\times T}$ denotes the matrix with all T received training signals from all M RX antennas in baseband. The term $\mathbf{N} \in \mathbb{C}^{M\times T}$ represents the complex AWGN matrix that is distributed as $\mathbf{N} \sim \mathcal{N}(\mathbf{0}_{M\times T}, \sigma^2\mathbf{I}_M)$. The matrix $\mathbf{\Phi} \in \mathbb{C}^{MNL_p\times MNL_pKT}$ is built using the training symbols q_n's, as:

$$\mathbf{\Phi} \triangleq [\mathbf{I}_M \otimes \mathrm{blkdiag}\left((\mathbf{I}_{L_p} \otimes \mathbf{q}_1^{\mathrm{T}}(1)), \ldots, (\mathbf{I}_{L_p} \otimes \mathbf{q}_N^{\mathrm{T}}(1))\right), \ldots \\ \mathbf{I}_M \otimes \mathrm{blkdiag}\left((\mathbf{I}_{L_p} \otimes \mathbf{q}_1^{\mathrm{T}}(T)), \ldots, (\mathbf{I}_{L_p} \otimes \mathbf{q}_N^{\mathrm{T}}(T))\right)]. \tag{23}$$

Finally, the binary matrix $\mathbf{E} \in \{0,1\}^{MNL_pKT\times T}$ in (22) is introduced to represent the unknown time shifts and is defined as follows:

$$\mathbf{E} \triangleq \mathbf{I}_T \otimes \mathbf{e}. \tag{24}$$

Finally, we formulate our channel estimation objective incorporating the dual-wideband effect as the following optimization problem:

$$\begin{aligned}\mathcal{OP}: \min_{\mathbf{K},\mathbf{e}} &\|\mathbf{Y}-\mathbf{K}\mathbf{\Phi}(\mathbf{I}_T\otimes\mathbf{e})\|_{\mathrm{F}}^2\\ &\text{s.t. } [\mathbf{e}]_p\in\{0,1\}\ \forall p=1,\ldots,MNL_pK,\\ &\text{and } \mathbf{K} \text{ as in (20).}\end{aligned} \tag{25}$$

Remark: $\mathcal{OP}$ is categorized as a *biconvex* optimization problem, wherein the two unknowns, $\mathbf{K}$ and $\mathbf{e}$, are involved through their product in the objective function. More specifically, the problem is classified as mixed-integer since $\mathbf{e}$ is an element of the binary subset.

C. Solution

An effective approach to tackle a biconvex problem is to decompose it into two independent subproblems, which can then be solved separately:

- Given that the channel matrix is perfectly known, denoted as $\mathbf{K}^*$, solve for the beam-squint vector $\mathbf{e}$:

$$\begin{aligned}\mathcal{OP}_1: \mathbf{e}_{\text{est}} \triangleq \arg\min_{\mathbf{e}} &\|\mathbf{Y}-\mathbf{K}^*\mathbf{\Phi}(\mathbf{I}_N\otimes\mathbf{e})\|_{\mathrm{F}}^2\\ &\text{s.t. } [\mathbf{e}]_p\in\{0,1\}.\end{aligned} \tag{26}$$

  Problem $\mathcal{OP}_1$ can be addressed by replacing the integer constraint with a sparsity-promoting norm operator, i.e., L1-norm into the cost function. To do so, we define vector $\tilde{\mathbf{e}} \in [0,1]^{MNKL_p\times 1}$ with $[\tilde{\mathbf{e}}]_q \in [0,1]$ with $q=1,2,\ldots,MNKL_p$, and observing that the number of the non-zero elements are equal to the product MNL. Thus, $\mathcal{OP}_1$ becomes

$$\begin{aligned}&\min_{\tilde{\mathbf{e}}}\|\tilde{\mathbf{e}}\|_1+\frac{1}{2}\|\text{vec}(\mathbf{Y})-(\mathbf{I}\otimes\mathbf{K}^*\mathbf{\Phi})\text{vec}(\mathbf{I}_T\otimes\tilde{\mathbf{e}})\|_2^2\\ &\text{s.t.}\|\tilde{\mathbf{e}}\|_2=MNL_p,\end{aligned} \tag{27}$$

  which is easily solved using available toolboxes (e.g., CVX). Afterwards, a thresholding function is applied to the output, i.e.,

$$[\mathbf{e}_{\text{est}}]_q=\text{thres}([\tilde{\mathbf{e}}]_q)\in\{0,1\}, \tag{28}$$

  with $q=1,2,\ldots,MNKL_p$.
- Given that the binary vector $\mathbf{e}_{\text{est}}$, solve for $\mathbf{K}$:

$$\begin{aligned}\min_{\mathbf{K}} &\|\mathbf{Y}-\mathbf{K}\mathbf{\Phi}(\mathbf{I}_N\otimes\mathbf{e}_{\text{est}})\|_{\mathrm{F}}^2\\ &\text{s.t. } \mathbf{K} \text{ as in (20).}\end{aligned} \tag{29}$$

  The closed-form solution of the unconstrained problem (29) is expressed as:

$$\tilde{\mathbf{K}}_{\text{est}}=\mathbf{Y}(\mathbf{\Phi}\mathbf{E}_{\text{est}})^{\dagger}, \tag{30}$$

  with $\mathbf{E}_{\text{est}}=\mathbf{I}_N\otimes\mathbf{e}_{\text{est}}$. Subsequently, we impose the block configuration described in (20),

$$\mathbf{K}_{\text{est}}=\mathcal{P}(\tilde{\mathbf{K}}_{\text{est}}). \tag{31}$$

In this study, we consider an ideal case of perfect initialization, allowing the two subproblems to be solved in a single step. However, in a more practical setting, an alternating minimization approach would be preferable to progressively reduce errors arising from imperfect initialization.

The overall *computational complexity* involves primarily two key calculations: First, the binary vector $\mathbf{e}_{\text{est}}$ is calculated by solving $\mathcal{OP}_1$ and thresholding, costing $\mathcal{O}(MNL_p)$. Second, the channel matrix $\mathbf{K}$ is inverted, leading to a general complexity of $\mathcal{O}((MNL_p)^3)$. However, this can be lowered down to $\mathcal{O}((MNL_p)^{3/2})$ by leveraging its sparse structure.

IV. Simulation Results and Discussion

We assume that the considered point-to-point communication system takes place for distances larger than the Fraunhofer distance. According to the SC modulation under consideration, the TX communicates with the UE via data-carrying frames, where each frame is composed by T time instances allocated for the training symbols. Thus, for $t=1,2,\ldots,T$, the TX transmits the training symbols $q_n(t)\sim\mathcal{CN}(0,1)$. The default system parameters was set to $N=M=32$, $T=500$. In our simulation, we employ MUSIC algorithm to estimate the AoAs, assuming that the channel gains, as well as the number of the propagation paths (model-order), are perfectly known. Also, we name as L1 method, the case that we solve (27) without taking into account the proposed constraint.

In Fig. 1 (left plot), we present the normalized mean square error (MSE) as a function of the Signal-to-Noise Ratio (SNR $\triangleq 1/\sigma^2$), comparing the performance of standard techniques, such as Least-squares, OFDM, and MUSIC, with the proposed approach. The Least-squares method estimates the channel matrix $\mathbf{K}$ and the binary matrix $\mathbf{E}$. However, it is structure-agnostic and requires a large number of pilot symbols for accurate estimation. MUSIC, on the other hand, disregards the channel gain and focuses solely on computing the AoA. For OFDM, the channel variation across subcarriers limits its performance, as the available pilots are distributed across all subcarriers, resulting in constrained accuracy.

Figure 2 illustrates the performance of three methods in recovering the true values of the binary vector $\mathbf{e}$: Least-squares, L1, and our proposed technique. Least-squares suffers from significant inaccuracies, while L1 and our method effectively locate the non-zero elements. However, our method distinguishes itself by achieving recovered values that are closer to the ideal unity. To further evaluate the performance, Figure 1 (right plot) compares the techniques based on the MSE metric for binary vector estimation over different SNR values.

Figure 3 showcases the performance of the techniques for different environments, such as Urban Micro (UMi) and Macro (UMa), as well as Rural Macro (RMa). Each environment sets different values for the number of the propagation paths L_p and the maximum delay time K. Specifically, for UMi we set the number of propagation paths $L_p=1$ and maximum delay time $K=5$; for UMa $L_p=2$ and $K=15$, while for RMa $L_p=3$ and $K=25$. With known bandwidth, sampling rate, and carrier frequency, the values of the maximum delay parameter K can be expressed in time units. The results

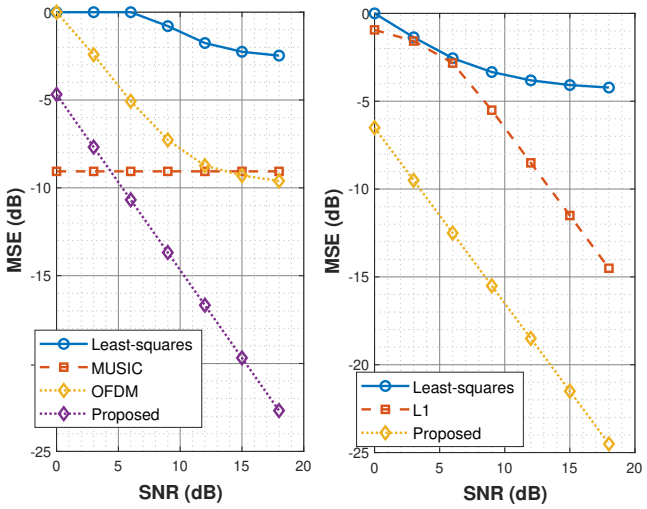

Fig. 1. Evaluation of the channel matrix $\mathbf{K}_{\text{est}}$ (left plot) and the binary vector $\mathbf{e}_{\text{est}}$ (right plot) estimation accuracy.

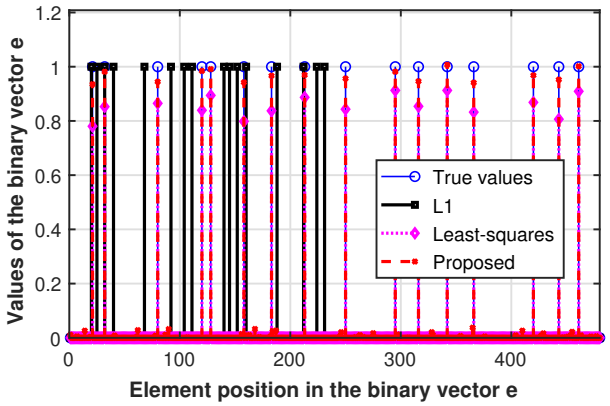

Fig. 2. Illustration of the techniques' ability to accurately identify the non-zero components, with SNR= 20 dB.

confirm that the technique effectively minimizes MSE in various environments, and as expected, the MSE scales with the difficulty of the environment.

REFERENCES

[1] B. Wang, M. Jian, F. Gao, G. Y. Li, and H. Lin, "Beam Squint and Channel Estimation for Wideband mmWave Massive MIMO-OFDM Systems," *IEEE Transactions on Signal Processing*, vol. 67, no. 23, pp. 5893–5908, 2019.

[2] Y. Lin, S. Jin, M. Matthaiou, and X. You, "Tensor-Based Channel Estimation for Millimeter Wave MIMO-OFDM With Dual-Wideband Effects," *IEEE Transactions on Communications*, vol. 68, no. 7, pp. 4218–4232, 2020.

[3] I.-S. Kim and J. Choi, "Spatial Wideband Channel Estimation for mmWave Massive MIMO Systems With Hybrid Architectures and Low-Resolution ADCs," *IEEE Transactions on Wireless Communications*, vol. 20, no. 6, pp. 4016–4029, 2021.

[4] W. Yu, Y. Shen, H. He, X. Yu, S. Song, J. Zhang, and K. B. Letaief, "An Adaptive and Robust Deep Learning Framework for THz Ultra-Massive MIMO Channel Estimation," *IEEE Journal of Selected Topics in Signal Processing*, vol. 17, no. 4, pp. 761–776, 2023.

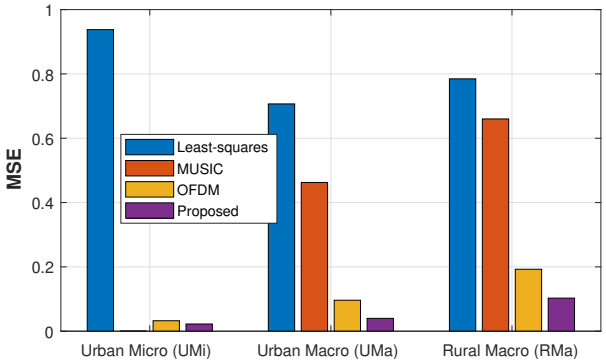

Fig. 3. Evaluation of the channel matrix $\mathbf{K}_{\text{est}}$ for different environments.

[5] W. Huang, Y. Huang, R. Zhao, S. He, and L. Yang, "Wideband millimeter wave communication: Single carrier based hybrid precoding with sparse optimization," *IEEE Transactions on Vehicular Technology*, vol. 67, no. 10, pp. 9696–9710, 2018.

[6] S. Buzzi, C. D'Andrea, T. Foggi, A. Ugolini, and G. Colavolpe, "Single-Carrier Modulation Versus OFDM for Millimeter-Wave Wireless MIMO," *IEEE Transactions on Communications*, vol. 66, no. 3, pp. 1335–1348, 2018.

[7] S. Srivastava, P. Sharma, S. Dwivedi, A. K. Jagannatham, and L. Hanzo, "Fast Block LMS Based Estimation of Angularly Sparse Channels for Single-Carrier Wideband Millimeter Wave Hybrid MIMO Systems," *IEEE Transactions on Vehicular Technology*, vol. 70, no. 1, pp. 666–681, 2021.

[8] S. Tarboush, H. Sarieddeen, M.-S. Alouini, and T. Y. Al-Naffouri, "Single- Versus Multicarrier Terahertz-Band Communications: A Comparative Study," *IEEE Open Journal of the Communication Society*, vol. 3, pp. 1466–1486, 2022.

[9] V. Schram, A. Moldovan, and W. H. Gerstacker, "Compressive Sensing for Indoor THz Channel Estimation," in *2018 52nd Asilomar Conference on Signals, Systems, and Computers*, 2018, pp. 1539–1546.

[10] E. Vlachos, G. C. Alexandropoulos, and J. Thompson, "Wideband MIMO channel estimation for hybrid beamforming millimeter wave systems via random spatial sampling," *IEEE J. Sel. Topics Signal Process.*, vol. 13, no. 5, pp. 1136–1150, Sep. 2019.

[11] V. Petrov, T. Kurner, and I. Hosako, "Ieee 802.15.3d: First standardization efforts for sub-terahertz band communications toward 6g," *IEEE Communications Magazine*, vol. 58, no. 11, pp. 28–33, 2020.

[12] H. Sarieddeen, M.-S. Alouini, and T. Y. Al-Naffouri, "An Overview of Signal Processing Techniques for Terahertz Communications," *Proceedings of the IEEE*, vol. 109, no. 10, pp. 1628–1665, 2021.

[13] C. Han, Y. Wang, Y. Li, Y. Chen, N. A. Abbasi, T. Kürner, and A. F. Molisch, "Terahertz Wireless Channels: A Holistic Survey on Measurement, Modeling, and Analysis," *IEEE Communications Surveys & Tutorials*, vol. 24, no. 3, pp. 1670–1707, 2022.

[14] S. Matos, Y. Ma, Q. Luo, J. Deuermeier, L. Lucci, P. Gavriilidis, A. Kiazadeh, V. Lain-Rubio, T. D. Phan, P. J. Soh, A. Clemente, L. M. Pessoa, and G. C. Alexandropoulos, "Reconfigurable Intelligent Surfaces for THz: Hardware Impairments and Switching Technologies," in *2024 IEEE International Conference on Electromagnetic Advanced Applications (ICEAA)*, Lisbon, Portugal, 2024.

[15] A. Saleh and R. Valenzuela, "A Statistical Model for Indoor Multipath Propagation," *IEEE J. Sel. Areas Commun.*, vol. 5, no. 2, pp. 128–137, 1987.

[16] D. Tse and P. Viswanath, *Fundamentals of Wireless Communication*. Cambridge: Cambridge University Press, 2005.